Translational Oncology 14 (2021) 101034

Contents lists available at ScienceDirect

Translational Oncology

journal homepage: www.elsevier.com/locate/tranon

Machine-learning analysis of contrast-enhanced computed tomography radiomics predicts patients with hepatocellular carcinoma who are unsuitable for initial transarterial chemoembolization monotherapy: A multicenter study

Zhicheng Jin[a,1], Li Chen[a,1], Binyan Zhong[b,1], Haifeng Zhou[c,1], Haidong Zhu[a,1], Hai Zhou[a], Jingjing Song[d], Jinhe Guo[a], Xiaoli Zhu[b], Jiansong Ji[d,*], Caifang Ni[b,*], Gaojun Teng[a,*]

[a] Center of Interventional Radiology and Vascular Surgery, Department of Radiology, Zhongda Hospital, Medical School, Southeast University, Nanjing 210009, China
[b] Department of Interventional Radiology, The First Affiliated Hospital of Soochow University, Suzhou, China
[c] Department of Interventional Radiology, The First Affiliated Hospital of Nanjing Medical University, 300 Guangzhou Road, Nanjing 210029, China
[d] Department of Interventional Radiology, Zhejiang University Lishui Hospital, The Fifth Affiliated Hospital of Wenzhou Medical University, Lishui Central Hospital, Lishui, China

ARTICLE INFO

Keywords:
Hepatocellular carcinoma
Transarterial chemoembolization
Radiomics
Unsuitable
Extrahepatic spread
Vascular invasion

ABSTRACT

Introduction: Due to the high heterogeneity of hepatocellular carcinoma (HCC), patients with non-advanced disease who are unsuitable for initial transarterial chemoembolization (TACE) monotherapy may have the potential to develop extrahepatic spread or vascular invasion. We aimed to develop and independently validate a radiomics-based model for predicting which patients will develop extrahepatic spread or vascular invasion after initial TACE monotherapy (EVIT).

Materials and methods: This retrospective study included 256 HCC patients (training set: $n = 136$; testing set: $n = 120$) who underwent TACE as initial therapy between April 2007 and June 2018. Clinicoradiological predictors were selected using multivariate logistic regression and a clinicoradiological model was constructed. The radiomic features were extracted from contrast-enhanced computed tomography (CT) images and a radiomics signature was constructed based on a machine learning algorithm. A combined model integrated clinicoradiological predictor and radiomics signature was developed. The predictive performance of the two models was evaluated and compared based on its discrimination, calibration, and clinical usefulness.

Results: In the training set, 34 (25.0%) patients were confirmed to have EVIT, whereas 26 (21.7%) patients in the testing set had EVIT. When the radiomics signature was added, the combined model showed improved discrimination performance compared to the clinicoradiological model (area under the curves [AUCs] 0.911 vs. 0.772 in the training set; AUCs 0.847 vs. 0.746 in the testing set) and could divide HCC patients into three strata of low, intermediate, or high risk in the two sets. Decision curve analysis demonstrated that the two models were clinically useful, and the combined model provided greater benefits for discriminating patients than the clinicoradiological model.

Conclusions: This study presents a model that integrates clinicoradiological predictors and CT-based radiomics signature that could provide a preoperative individualized prediction of EVIT in patients with HCC.

Introduction

Transarterial chemoembolization (TACE) is the most widely applied primary treatment for unresectable hepatocellular carcinoma (HCC) in clinical practice [1]. According to the BRIDGE study, it is widely used not only for intermediate-stage HCC, which is the standard recommendation based on the Barcelona Clinic Liver Cancer (BCLC) staging system, but also for advanced and selected cases of early stage HCC [1–3]. Due to its high heterogeneity, the prognosis of TACE for HCC varies, with the time to progression varying from 31 months to 135 months

Abbreviations: HCC, hepatocellular carcinoma; TACE, transarterial chemoembolization; CT, computed tomography; EVIT, extrahepatic spread or vascular invasion after initial; TACE, monotherapy; OS, overall survival; CI, confidence interval, IQR, interquartile range.

* Corresponding author.
E-mail addresses: jjstcty@sina.com (J. Ji), cjr.nicaifang@vip.163.com (C. Ni), gjteng@vip.sina.com (G. Teng).

[1] Zhicheng Jin, Li Chen, Binyan Zhong, Haifeng Zhou, Haidong Zhu contributed equally to this study.

https://doi.org/10.1016/j.tranon.2021.101034
Received 26 November 2020; Received in revised form 15 January 2021; Accepted 28 January 2021
1936-5233/© 2021 Published by Elsevier Inc. This is an open access article under the CC BY-NC-ND license (http://creativecommons.org/licenses/by-nc-nd/4.0/)

[4]. Patients who are unsuitable for TACE could experience progression in the form of extrahepatic spread or vascular invasion after initial TACE monotherapy (EVIT) [5,6]. This is more likely to be caused by the complex heterogeneity of the tumor microenvironment, rather than a failure of the TACE procedure [7,8]. For these patients, combination treatment with TACE and systemic therapy (molecular targeted therapy or immunotherapy) should be considered rather than TACE monotherapy [9,10].

Radiomics is the high-throughput extraction of quantitative features from medical images that could reflect underlying tissue and lesion characteristics, such as tumor heterogeneity, in a non-invasive way [11–13]. Radiomics analyses with favorable predictive value for the therapeutic response and prognosis of TACE have been reported [14–16]. Most radiomics models based on the preoperative image predict patients' long-term outcomes, which are affected by various factors that may weaken the actual predictive performance. Few of these studies have been validated by independent external institutions. To the best of our knowledge, no multicenter studies have created a radiomics-based model for predicting initial TACE-unsuitable patients to improve the management of HCC.

This study aimed to develop a model integrating clinical, radiologic, and radiomic features to preoperatively predict extrahepatic spread or vascular invasion for non-advanced HCC patients initially treated with TACE monotherapy. The prognostic and predictive efficacy of the model was also evaluated externally in the independent testing set.

Materials and methods

Patients

This retrospective study was conducted in patients with unresectable HCC who underwent TACE between April 2007 and June 2018 at three institutions in China. The study protocol conformed to the ethical guidelines of the 1975 Declaration of Helsinki. The study was approved by the institutional ethics review boards of the three participating institutions(2019ZDSYLL069-P01), and the requirement for written informed consent was waived due to the retrospective nature of the study.

The inclusion criteria were as follows: (a) aged 18 years or older; (b) diagnosed with HCC according to the European Association for the Study of the Liver (EASL) [1] or the American Association for the Study of Liver Disease (AASLD) [2] criteria; (c) Eastern Cooperative Oncology Group (ECOG) performance status of 0; (d) Child-Pugh grade A or B; (e) unable or unwilling to undergo surgical resection or ablation; and (f) no extrahepatic spread or vascular invasion. The exclusion criteria were: (a) lack of preoperative contrast-enhanced computed tomography (CT) imaging; (b) previous HCC-related treatment; (c) Child-Pugh C liver function or evidence of decompensated liver cirrhosis including refractory ascites, esophageal or gastric variceal bleeding, or hepatic encephalopathy; and (d) missing follow-up data or lost to follow-up.

For each patient, demographics, hepatitis history, Child–Pugh class, preoperative liver function tests, and serum alpha-fetoprotein (AFP) levels were collected from medical records. Finally, a total of 256 patients were included (51 women and 205 men; median age, 60.5 years; interquartile range, 52–71 years) and divided into a training set (institution 1 & 2, $n = 136$; 28 women and 108 men; median age, 60 years; interquartile range, 52–67 years) and an independent external testing set (institution 3, $n = 120$; 23 women and 97 men; median age, 61 years; interquartile range, 53–73 years), as shown in Fig. 1.

Assessment

All patients underwent routine abdominal contrast-enhanced CT and plain chest CT scans; other CT scans were then conducted according to individual conditions. According to the EASL guidelines, the extrahepatic spread was defined as lymph node involvement or extrahepatic metastases, and vascular invasion was defined as macrovascular invasion either segmental or portal invasion [1]. Only if there was no definite extrahepatic spread or vascular invasion in the preoperative CT imaging, EVIT on follow-up imaging could be determined. Patients thought to have preoperative extrahepatic spread or vascular invasion were considered to have advanced HCC and were excluded from the study.

The radiologic characteristics of tumors were assessed by two independent radiologists (reader 1 and reader 2, with 10 and 15 years of abdominal imaging experience) who were blinded to the patients' information. The radiologic features of HCC, partly referring to Elsayes et al. [17] and Yoneda et al. [18], included (a) tumor number, the number of visible lesions; (b) tumor size, defined as the diameter of the largest lesion; (c) enhancement pattern, classified as typical dynamic enhancement with arterial-phase hyperenhancement, and washout in portal-venous phase or delay phase, or atypical dynamic enhancement; (d) tumor capsule, defined as a smooth, uniform border surrounding the mass and visible as an enhancing rim on portal venous or delayed phase imaging, or non-enhancing rim; (e) uni- or multilobar involvement; (f) tumor margin, classified as nodular HCC with a smooth margin or non-nodular HCC with an irregular border; (g) arterial peritumoral enhancement, defined as transient hepatic parenchymal enhancement adjacent to the tumor border in the arterial phase and return to normal in the portal vein phase; (h) intratumor necrosis, classified as absent or present; and (i) intratumor hemorrhage, classified as absent or present. When patients had multiple nodules, the largest nodule was analyzed. Any disagreement between radiologists was discussed to reach a final consensus.

TACE procedure and follow-up

All patients included in the study underwent the conventional TACE procedure performed by several interventional radiologists (with >20 years of experience). The emulsion of chemotherapeutic drugs (pirarubicin, epirubicin, or cisplatin was selected according to the practice of each center) and lipiodol, the dosages of which were determined by the tumor size and vascularity, was injected into feeding arteries of the tumor followed by gelatin sponge particles. The TACE procedure was carried out in a superselective manner to increase efficacy and reduce complications. The patients were followed-up using dynamic CT or magnetic resonance imaging (MRI) at 4–8 weeks after TACE. Subsequent TACE procedures were performed "on demand": If a residual tumor or new intrahepatic lesions were demonstrated, the patient was evaluated for repeated TACE treatment. Systemic therapy or combined therapy was considered when vascular invasion and extrahepatic spread were present.

CT image acquisition

All contrast-enhanced CT examinations were performed within 1 month before TACE. The detailed imaging protocols are shown in the Supplementary methods.

Tumor segmentation and radiomic feature extraction

The workflow of the radiomics analysis is shown in Fig. 1. Three-dimensional manual segmentation was performed by a radiologist (reader 1) using ITK-SNAP software (version 380, www.itksnap.org) [19]. The regions of interest were drawn on portal venous phase images, slice by slice. To standardize the voxel spacing, all images were resampled to a voxel size of $1 \times 1 \times 3$ mm. Thereafter, we used a fixed bin width to discretize voxel intensity values to control image noise and normalize voxel intensities. In total, 1218 radiomic features (detailed in the Supplementary methods) including shape ($n = 14$), first-order ($n = 18$), texture ($n = 68$), Laplacian of Gaussian (LoG, $n = 430$), and wavelet ($n = 688$) features were extracted automatically from each segmented region of interest using the open-source Pyradiomics package

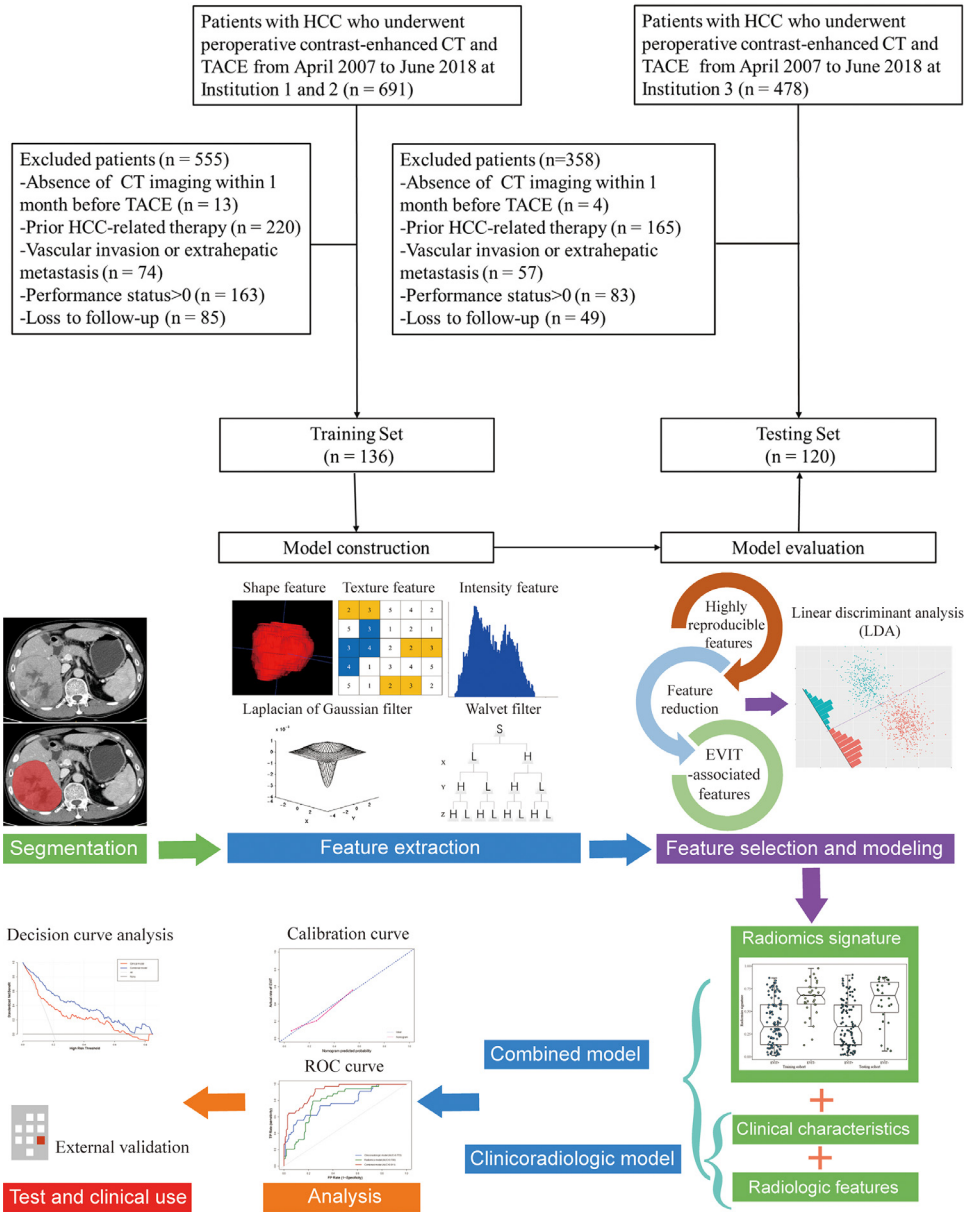

Fig. 1. Flow chart of study design (top) and workflow of radiomics analysis (below). HCC, hepatocellular carcinoma; TACE, transarterial chemoembolization; CT, computed tomography.

(version 2.2.0; https://github.com/Radiomics/pyradiomics) [20]. The reproducibility of inter-observer segmentation was confirmed by two radiologists (reader 1 and reader 2). Interclass correlation coefficients (ICC) values greater than 0.8 were considered for further investigation.

Radiomic feature selection and signature building

The feature matrix was normalized by scaling to the unit length method. For scaling the components of a feature vector, each component was divided by the Euclidean length of each vector. The feature vector was then mapped to a unit vector. Pearson correlation coefficients were used to reduce dimensionality, and analysis of variance was used for selecting relevant features. Linear discriminant analysis (LDA) was used as the linear classifier by fitting class conditional densities to the data and using Bayes' rule to build a radiomics model. Meanwhile, the internal validation set was separated from the training set by 10-fold cross-validation to adjust the model parameters and prove the performance of the model. All of the above radiomic analysis processes were implemented using an open-source software package, FeAture Explorer (FAE, version 0.2.7; https://github.com/salan668/FAE) [21]. The radiomics model was converted into a probability score, namely the radiomics signature, indicating the individual relative risk for EVIT.

Model building, performance, validation, and comparison

For the clinicoradiological risk factors, univariate and multivariate logistic regression analyses were applied to determine the predictors of EVIT in the training set. The clinicoradiological nomogram model was built based on the results of the logistic multivariate analysis, and the combined nomogram model was established based on the clinicoradiological nomogram model and radiomics signature. The discrimination performance of the two models was measured using the receiver-operating characteristic (ROC) curve based on the area under the curve (AUC), sensitivity, specificity, and accuracy. Calibration curves were drawn to compare the probability of EVIT between the predicted and actual rates according to the Hosmer-Lemeshow test. Comparisons of the AUCs of the ROC curves were performed using the Delong test. The performance improvement introduced by the inclusion of the radiomics signature was quantified using net reclassification improvement (NRI) and integrated discrimination improvement (IDI). The clinical useful-

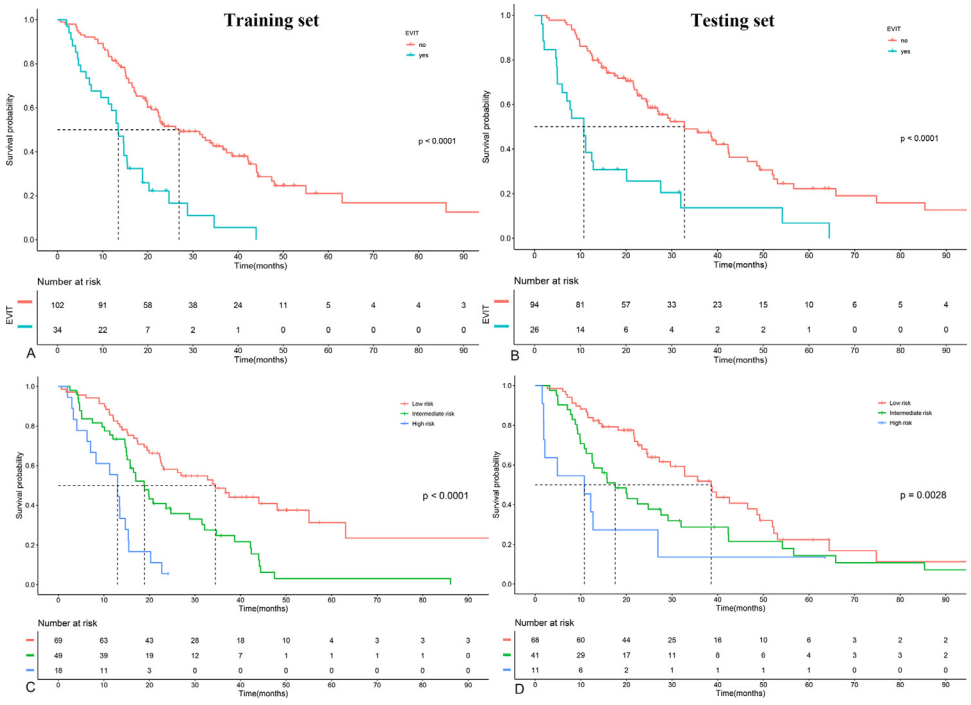

Fig. 2. Survival curves according to EVIT status (A, B), and risk strata identified using the combined model (C, D) for the training and test sets, respectively. Patients without EVIT had a longer OS than patients with EVIT in the training set (p<0.001; A) and the testing set (p<0.001; B). The combined models stratified patients into three risk strata (median OS, 34.5 months, 18.9 months, and 13.0 months for low-, intermediate-, high-risk patients in the training set, respectively, p < 0.001; median OS, 38.6 months, 17.6 months, and 10.8 months, for low-, intermediate-, high-risk patients in the testing set, respectively, p = 0.003). OS, overall survival; EVIT, extrahepatic spread or vascular invasion after initial TACE monotherapy.

ness of the two nomograms was evaluated using decision curve analysis (DCA) by calculating the net benefit at different threshold probabilities.

Statistical analysis

Continuous variables were compared using Student's t-test or non-parametric Mann-Whitney U test, and categorical variables were compared using the chi-squared test or Fisher exact test. Overall survival (OS) was defined as the interval from the date of the initial TACE procedure to the date of all-cause death. Patients who survived until the last follow-up date (March 18th, 2020) or were lost to follow-up were censored. Survival curves were constructed using the Kaplan-Meier method and compared using a two-sided log-rank test. The X-tile software (version 3.6.1; Yale University School of Medicine, USA) in the training set to determine the optimal cutoff value for risk score output from the combined predictive model. A p-value ≤0.05 was considered statistically significant. All statistical analyses were performed using SPSS (version 210; IBM, Somers, NY) and R software (version 3.63; R Project for Statistical Computing, http://www.r-project.org).

Results

Clinicoradiological characteristics

The baseline clinical and radiologic characteristics of all patients are shown in Table 1. Among them, 60 (23.4%) patients with EVIT were confirmed on follow-up imaging (34 [25.0%] in the training set, 26 [21.7%] in the testing set). The median follow-up interval after initial TACE was 47.0 days (IQR: 37.0–61.0) in the training set and 47.0 days (IQR: 37.3–62.5) in the testing set (p = 0.890). The median OS in the training set for patients with EVIT was 13.5 (95%CI: 11.3–18.8) months, compared with 26.9 (95%CI: 22.2–38.7) months in patients without EVIT (p < 0.001). Significant differences in median OS were also seen in the testing set (10.8 [95%CI: 6.0–27.6] vs. 32.8 [95%CI: 24.8–46.6]; p < 0.001; Fig. 2).

After multivariate analysis, the baseline serum bilirubin level (OR 1.09; 95%CI 1.04–1.15; p < 0.001), tumor number (OR 1.54; 95%CI 1.16–2.03; p = 0.003), and tumor capsule (OR 0.23; 95%CI 0.08–0.64; p = 0.005) were independent predictors of EVIT (Table S1). Thereafter, a clinicoradiological prognostic nomogram was established to predict EVIT (Fig. 3). The AUCs for the clinicoradiological model was 0.772 (95% CI: 0.676–0.868) in the training set and 0.746 (95% CI: 0.641–0.852) in the testing set (Fig. 4). The calibration curves for the clinicoradiological model demonstrated good agreement between the predicted and observed probabilities for EVIT in both the training and testing sets (p = 0.580 and p = 0.722, respectively; Fig. 5).

Radiomic features and radiomics signature

Among the 1218 features, 1106 features with an interclass correlation coefficient >0.8 were stable for further analysis (Fig. S1). Using the LDA classifier, 14 radiomic features were used to construct a radiomics signature (Table S2). The radiomics signature was significantly associated with EVIT (p<0.001) and achieved a satisfying predictive performance, with an AUC of 0.790 (95%CI: 0.709–0.871) in the training set and 0.750 (95%CI: 0.640–0.861) in the testing set. The distribution of the radiomics signature for each patient in the two sets is shown in Fig S2.

Combined model construction and validation

The nomograms based on the combined EVIT prediction model developed by integrating clinicoradiological factors with radiomics signature are shown in Fig. 3. The model yielded an AUC of 0.911 (95%CI: 0.862–0.961) and 0.847 (95%CI: 0.775–0.919) for EVIT prediction in the training and testing sets, respectively (Fig 4). The sensitivity, specificity, and accuracy of the combined model were 94.1%, 74.5%, and 79.4% in the training set and 76.9%, 79.8%, and 79.2% in the testing set, respectively (Table 2). The calibration curves for the combined model demonstrated good agreement between the predicted and observed probabilities for EVIT in both the training and testing sets (p = 0.419 and p = 0.290, respectively; Fig 5). By using the X-tile-determined optimal cutoff points, the combined models stratified patients into three risk categories of OS (median OS, 34.5 months, 18.9 months, and 13.0 months for low-, intermediate-, high-risk patients in the training set, respectively, p < 0.001; 38.6 months, 17.6 months, and

Table 1
Baseline clinical and radiologic characteristics of patients.

Variable	Entire set ($n = 256$)	Training set ($n = 136$)	Testing set ($n = 120$)	p value
Sex				0.899
Female	51 (20)	28 (21)	23 (19)	
Male	205 (80)	108 (79)	97 (81)	
Age (yr)	60.5 (52–71)	60.0 (52–67)	61 (53–73)	0.359
Hepatitis infection				0.207
absent	51 (20)	30 (22)	21 (18)	
hepatitis B	197 (77)	104 (76)	93 (78)	
hepatitis C	8 (3)	2 (1)	6 (5)	
Child-Pugh grade				0.205
A	222 (87)	114 (84)	108 (90)	
B	34 (13)	22 (16)	12 (10)	
BCLC stage				0.060
A	101 (39.5)	61 (44.9)	40 (33.3)	
B	155 (60.5)	75 (55.1)	80 (66.7)	
NLR	2.59 (1.77–4.01)	2.66 (1.77–4.14)	2.51 (1.86–3.49)	0.335
ALB (g/L)	37.1 (34.0–41.0)	38.5 (34.5–42.1)	36.4 (32.3–40.0)	0.010
Serum bilirubin (μmol/L)	16.1 (11.2–22.4)	16.3 (11.2–22.3)	16.0 (11.2–21.4)	0.561
ALT (U/L)	35.5 (22.8–60)	35.0 (22.8–62.4)	37.0 (22.8–58.0)	0.770
AST (U/L)	44.0 (30–67.3)	48.3 (3.24–68.1)	40.0 (2.88–65.5)	0.132
AFP (ng/dl)				0.216
<200	144 (56)	83 (61)	61 (51)	
200-400	15 (6)	6 (4)	9 (8)	
>400	97 (38)	47 (35)	50 (42)	
Radiologic features				
Tumor number				0.032
1	92 (35.9)	62 (45.6)	30 (25.0)	
2	72 (28.1)	29 (21.3)	43 (35.8)	
3	27 (10.5)	9 (6.6)	18 (15.0)	
4	22 (8.6)	11 (8.1)	11 (9.2)	
≥5	43 (16.9)	25 (18.4)	18 (15.0)	
Tumor size (cm)	6.2 (3.8–10.2)	6.7 (4.2–10.2)	6.0 (3.4–10.3)	0.398
Arterial phase hyperenhancement				0.664
typical	192 (75.0)	104 (76.5)	88 (73.3)	
atypical	64 (25.0)	32 (23.5)	32 (26.7)	
Tumor capsule				0.313
absent	144 (56.3)	81 (59.6)	63 (52.5)	
present	112 (43.7)	55 (40.4)	57 (47.5)	
Multilobe involved				0.073
absent	165 (64.5)	95 (69.9)	70 (58.3)	
present	91 (35.5)	41 (30.1)	50 (41.7)	
Tumor margin				0.777
smooth	116 (45.3)	60 (44.1)	56 (46.7)	
nonsmooth	140 (54.7)	76 (55.9)	64 (53.3)	
Arterial peritumoral enhancement				0.939
absent	217 (84.8)	116 (85.3)	101 (84.2)	
present	39 (15.2)	20 (14.7)	19 (15.8)	
Intratumor necrosis				0.495
absent	81 (31.6)	40 (29.4)	41 (34.2)	
present	175 (68.4)	96 (70.6)	79 (65.8)	
Intratumor hemorrhage				0.060
absent	15 (5.9)	12 (8.8)	3 (2.5)	
present	241 (94.1)	124 (91.2)	117 (97.5)	

Note–Data are median (IQR), n (%). BCLC, Barcelona Clinic Liver Cancer; NLR, neutrophils/lymphocytes ratio; ALB, albumin; ALT, alanine transaminase; AST, aspartate transaminase; AFP = alpha-fetoprotein.

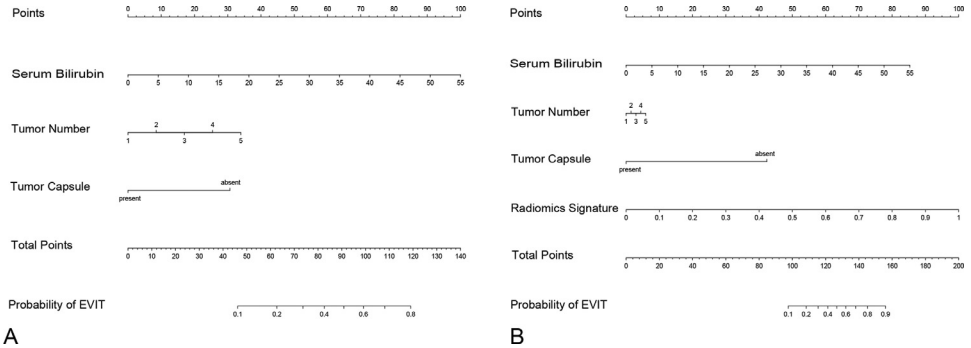

Fig. 3. Nomograms for the clinicoradiological and combined models. (A) Clinicoradiological nomogram based on three clinicoradiological predictors. (B) Combined nomogram based on three clinicoradiological predictors and radiomics signature.

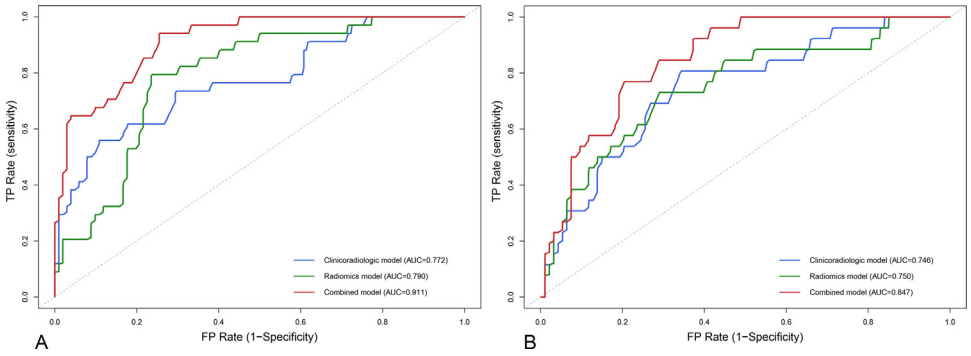

Fig. 4. Receiver operating characteristic curves with the area under the curve of the models in the training set (A) and testing set (B). FP, false positive; TP, true positive; AUC, area under the curve.

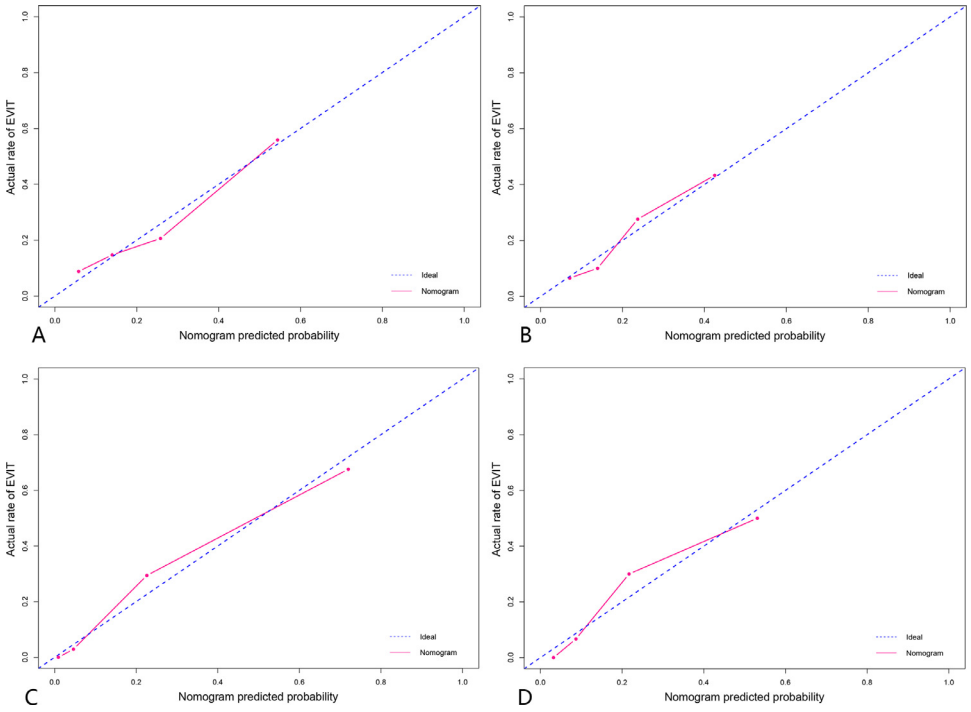

Fig. 5. Calibration curves for the predictive performance for EVIT. Clinicoradiological model in the training set (A, $p = 0.580$) and testing set (B, $p = 0.722$). Combined model in the training set (C, p=0.419) and testing set (D, $p = 0.290$). EVIT, extrahepatic spread or vascular invasion after initial TACE monotherapy.

10.8 months, for low-, intermediate-, high-risk patients in the testing set, respectively, $p = 0.003$; Fig 2).

Comparison between clinicoradiological model and combined model

The AUCs of the combined model were greater than the AUCs of the clinicoradiological model (0.911 vs. 0.772, $p < 0.001$, in the training set; 0.847 vs. 0.746, $p = 0.056$, in the testing set) and radiomics signature (0.911 vs. 0.790, $p < 0.001$, in the training set; 0.847 vs. 0.750, $p = 0.020$, in the testing set). In the testing set, the combined model showed better predictive performance than the clinicoradiological model, with no statistical difference. The detailed diagnostic performance of the clinicoradiological, radiomic, and combined EVIT prediction models are summarized in Table 2. The NRI and IDI of the combined model showed that the improvement over the clinicoradiological model in the training set was 0.38 (95%CI 0.15–0.62, $p = 0.001$) and 0.26 (95%CI, 0.18–0.34, $p < 0.001$), respectively; those of the testing set were 0.13 (95%CI -0.13 to 0.39, $p = 0.329$) and 0.12 (95%CI, 0.04–0.21, $p = 0.005$; Table 3), respectively. The DCA curves demonstrated that if the threshold probability is more than 5%, using the clinicoradiological and combined model to predict EVIT adds more benefit than either the treat-all scheme or treat-none scheme. If the threshold probability of a patient was between 2% and 85%, the net benefit in predicting EVIT using the combined model was superior to that of the clinicoradiological model (Fig 6).

Discussion

In this study, a radiomics-based combined model was developed and validated to incorporate serum total bilirubin, tumor capsule, tumor number, and radiomics signature for individualized, perioperative prediction of early- and intermediate-stage HCC patients who developed extrahepatic spread or vascular invasion after initial TACE monotherapy (EVIT). Meanwhile, a clinicoradiological model that incorporated serum bilirubin, tumor capsule, and tumor number was established to make a comparison with the radiomics-based combined model. The performance of the two models was validated with respect to discrimination, calibration, and clinical application in both the training and external testing sets. The combined model performed better than the clinicoradiological model. The median OS of patients with EVIT in our study, similar to the survival time of patients with advanced HCC, was significantly worse than that of patients without EVIT.

It is essential to identify HCC patients who are unsuitable for initial TACE monotherapy with a high potential to develop extrahepatic spread or vascular invasion. The initial treatment strategy should be changed in these patients who may benefit from early combined treatment with TACE and systemic therapy (lenvatinib/sorafenib, or immunotherapy)

Table 2
Performance of different models for EVIT.

Different models	Training set ($n = 136$)					Testing set ($n = 120$)				
	sensitivity, %	specificity, %	accuracy, %	AUC (95%CI)	*p* value*	sensitivity, %	specificity, %	accuracy, %	AUC (95%CI)	*p* value*
Clinicoradiolgic model	55.9	89.2	80.9	0.772 (0.676-0.868)	<0.001	80.8	66.0	69.1	0.746 (0641-0.852)	0.056
Radiomics signature	79.4	76.5	77.2	0.790 (0.709-0.871)	0.002	73.1	71.3	71.7	0.750 (0640-0.861)	0.020
Combined model	94.1	74.5	79.4	0.911 (0.862-0.961)	-	76.9	79.8	79.2	0.847 (0775-0.919)	-

* Delong test was used to compare the performance of models, between the radiomic model and combined model, clinicoradiologic and combined model. EVIT, extrahepatic spread or vascular invasion after initial TACE monotherapy; AUC, area under the curve.

Table 3
Comparison of combined and clinicoradiologic nomograms.

	NRI	95%CI	*P* value	IDI	95%CI	*P* value
Training set	0.38	0.15-0.62	0.001	0.26	0.18-0.34	<0.001
Testing set	0.13	-0.13–0.39	0.329	0.12	0.04–0.21	0.005

The performance improvement of the combined model compared with the clinicoradiologic model. NRI, net reclassification improvement; IDI, integrated discrimination improvement.

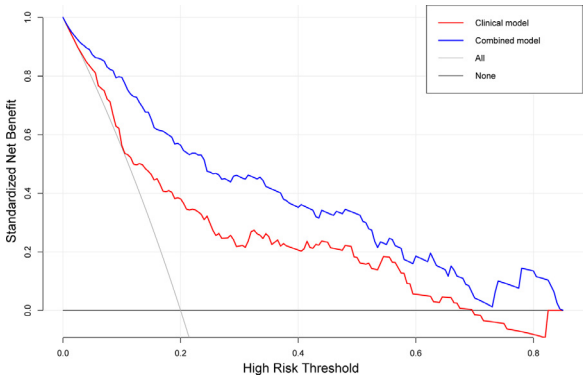

Fig. 6. Decision curve analysis of clinicoradiological and combined models for predicting EVIT. The y-axis measures the net benefits, wherein the red and blue line represents the clinicoradiological model and combined model, respectively. The gray line represents the assumption that all patients have EVIT presence. The black line represents the assumption that all patients have EVIT absence. It shows that the two models are better than the treat-all-patients scheme. While if the radiomics signature is added, it results in more benefits than the clinicoradiological model for patients' discrimination. EVIT, extrahepatic spread or vascular invasion after initial TACE.

[9]. The TACTICS trial demonstrated that the combination of TACE and sorafenib improves the clinical outcome of patients with intermediate HCC [22]. With an increasing number of systemic agents available in recent years, the optimal time for transition to systemic therapy and potential opportunities for combining TACE and systemic therapies has become a topic of debate. However, there is no broad consensus on when and in whom TACE therapy should be interrupted. The occurrence of extrahepatic spread or vascular invasion after TACE could be considered reflective of the clinical status of "untreatable progression" or "TACE failure/refractoriness" that requires the halting of TACE monotherapy at that time [1,23]. Therefore, the occurrence of extrahepatic spread or vascular invasion was selected as the endpoint of this study. We developed a combined model, incorporating clinicoradiological predictors and radiomics signature, to identify high-risk patients early to improve clinical decision making. The results of our study may provide a reference for patient inclusion criteria in future clinical trials that target combination treatment with TACE and systemic therapy, such as immunotherapy.

Without appropriate patient selection, TACE does not confer survival benefits. Nevertheless, in real-world clinical practice, TACE monotherapy is most frequently used as an initial therapy for unresectable HCC worldwide [3]. Thus, several studies have attempted to develop tools to optimize the appropriate selection of HCC patients for initial TACE. The Selection for TrAnsarterial chemoembolization TrEatment (STATE)-score was proposed and includes the preoperative serum albumin level, C-reactive protein level, and up to seven criteria trying to optimize the appropriate selection of HCC patients for initial TACE [24]. However, an external institution with 228 patients validated the STATE-score found that the STATE-score was unstable in determining the suitability for initial TACE [25]. A prospective observational study included 855 patients for investigating the long-term outcomes of different progression pat-

terns after initial TACE [5]. Among them, 17.1% of patients had early and intermediate stages of extrahepatic spread or vascular invasion.

Radiomics has been widely used as a non-invasive methodology in cancer research [12,13]. With an increasing number of clinical trials focusing on the combined use of systemic agents with TACE in the future, radiomics could provide cancer microenvironment information and be applied as a clinical biomarker. Our study demonstrates that the radiomic signature developed based on portal phase CT images could preoperatively predict EVIT patients with good performance. However, there could be a discrepancy in CT scanners and protocols in participating centers that may influence feature extraction. Voxel intensity discretization and voxel size resampling were used to minimize the dependency of radiomic features [12]. Normalization was applied on the gray level to improve the robustness of the features. By applying the LoG filter, glrlm_RunEntropy and glszm_ZoneEntropy indicate the heterogeneity of the texture patterns, while glcm_Idn and glcm_Idmn are measures of the local homogeneity of images (Table S2). The radiomic features selected could indicate tumor heterogeneity and are valuable for the prediction of prognostic factors and survival of TACE, which is consistent with previous radiomic analysis studies [15,16]. With the rapid development of radiogenomics and deep-learning technology, radiomics study could extract more key features and explore more possibilities in precision diagnostics and therapy in HCC.

Tumor burden was regarded as an important prognostic indicator quantified by the number and size of nodules [26]. A recent study showed that the number of nodules can better predict the prognosis of TACE instead of the size of nodules [27]. In our study, tumor number was an independent risk factor for EVIT. This finding aligns with the mechanism of multifocal HCC, which exhibited strong metastatic potential and diverse patterns of metastasis [28]. The proportion of solitary tumors in the training set was higher than that in the testing set, but this did not affect the reliability of the results. Regarding tumor burden-related factors, tumor size was statistically significant in the multivariate logistic regression of the clinicoradiological model. Nevertheless, the tumor size was removed from the two final models due to its negligible contribution.

Several previous studies found that HCC patients with a tumor capsule have a better prognosis after TACE [29,30]. Xu et al. reported that these patients had a higher 3- and 5-year survival rate (44.8 vs. 59.5% and 13.9 vs. 26.9%, respectively) [29]. However, false-negative image interpretations of the tumor capsule could occur, which may affect the nomogram's establishment and application, even if there was a final discussion between the two radiologists to reach a consensus. As a variable reflecting liver function, serum bilirubin was included in the ALBI grade and could achieve good patient stratification and discrimination [31]. For patients with higher baseline serum bilirubin levels and worse liver function, deterioration of hepatic function caused by TACE treatment may increase the risk of tumor metastasis and progression.

The combined model provided greater prediction benefits than the clinicoradiological model with good calibration in both sets. The improvement in NRI and IDI of the combined models show an increased proper reclassification and an increased probability of correct prediction. The DCA curves demonstrated that if the threshold probability is more than 5%, using the clinicoradiological and combined model to predict EVIT adds more benefit than either the treat-all scheme or treat-none scheme. The discrimination of the combined model was higher than that of the clinicoradiological model, with no statistical difference in the testing set (p = 0.056). The sensitivity of the combined model decreased from 80.8% in the clinicoradiological model to 76.9%. The combined model misjudged some negative cases as positive cases in the testing set, which reduced the true positive rate, subsequently affecting the discrimination and NRI of the model. However, this result does not compromise the effectiveness and robustness of the combined model for prognostic prediction.

Our study has several limitations. First, it is a retrospective study with a relatively small Asian population that suffers from inherent selection biases. The etiology of HCC in our study was mainly related to HBV, which differs from other regions where HCV- or alcohol-related HCC accounts for the majority of cases. Second, the radiomic features extracted from the arterial phase or delayed phase and feature changes between the two different phases were not exploited. These might be clinically significant because they correspond to the imaging pattern of HCC. Third, the radiologic interpretation of the tumor capsule could potentially be considered subjective.

Conclusion

This study presents the radiomic features of contrast-enhanced CT imaging and clinicoradiological risk factors that could preoperatively predict early- and intermediate-stage HCC patients who are likely to develop extrahepatic spread or vascular invasion after initial TACE monotherapy. To identify the worst candidates for initial TACE monotherapy, the radiomics-based combined model and clinicoradiological model may provide particular predictive value.

Declaration of Competing Interest

The authors declare that they have no known competing financial interests or personal relationships that could have appeared to influence the work reported in this paper.

Supplementary materials

Supplementary material associated with this article can be found, in the online version, at doi:10.1016/j.tranon.2021.101034.

CRediT authorship contribution statement

Zhicheng Jin: Conceptualization, Methodology, Software, Formal analysis, Data curation, Investigation, Writing - original draft, Writing - review & editing. **Li Chen:** Conceptualization, Methodology, Investigation, Data curation, Resources, Writing - review & editing. **Binyan Zhong:** Conceptualization, Methodology, Investigation, Data curation, Formal analysis, Writing - review & editing, Visualization. **Haifeng Zhou:** Conceptualization, Methodology, Software, Formal analysis, Writing - review & editing, Visualization. **Haidong Zhu:** Resources, Investigation, Writing - review & editing. **Hai Zhou:** Data curation, Investigation, Visualization. **Jingjing Song:** Data curation, Investigation, Resources. **Jinhe Guo:** Validation, Resources. **Xiaoli Zhu:** Validation, Resources. **Jiansong Ji:** Validation, Resources, Supervision, Project administration. **Caifang Ni:** Validation, Resources, Supervision, Project administration. **Gaojun Teng:** Conceptualization, Resources, Writing - review & editing, Supervision, Project administration, Funding acquisition.

References

[1] EASL clinical practice guidelines: management of hepatocellular carcinoma, J. Hepatol. 69 (1) (2018) 182–236.
[2] JK Heimbach, LM Kulik, RS Finn, et al., AASLD guidelines for the treatment of hepatocellular carcinoma, Hepatology (Baltimore, Md) 67 (1) (2018) 358–380.
[3] JW Park, M Chen, M Colombo, et al., Global patterns of hepatocellular carcinoma management from diagnosis to death: the BRIDGE Study, Liver Int. 35 (9) (2015) 2155–2166.
[4] R Lencioni, T de Baere, MC Soulen, WS Rilling, JF. Geschwind, Lipiodol transarterial chemoembolization for hepatocellular carcinoma: A systematic review of efficacy and safety data, Hepatology (Baltimore, Md) 64 (1) (2016) 106–116.
[5] YI Kim, JW Park, HW Kwak, et al., Long-term outcomes of second treatment after initial transarterial chemoembolization in patients with hepatocellular carcinoma, Liver Int. 34 (8) (2014) 1278–1286.
[6] CJ Kim, HJ Kim, JH Park, et al., Radiologic response to transcatheter hepatic arterial chemoembolization and clinical outcomes in patients with hepatocellular carcinoma, Liver Int. 34 (2) (2014) 305–312.
[7] DF Quail, JA. Joyce, Microenvironmental regulation of tumor progression and metastasis, Nat. Med. 19 (11) (2013) 1423–1437.
[8] X Wei, L Zhao, R Ren, et al., MiR-125b loss activated HIF1α/pAKT loop, leading to trans-arterial chemoembolization resistance in hepatocellular carcinoma, Hepatology (Baltimore, Md) (2020).

[9] M Kudo, KH Han, SL Ye, et al., A changing paradigm for the treatment of intermediate-stage hepatocellular carcinoma: Asia-pacific primary liver cancer expert consensus statements, Liver Cancer 9 (3) (2020) 245–260.
[10] S De Lorenzo, F Tovoli, M Barbera, et al., Metronomic capecitabine vs. best supportive care in Child-Pugh B hepatocellular carcinoma: a proof of concept, Sci. Rep. 8 (1) (2018) 9997.
[11] P Lambin, E Rios-Velazquez, R Leijenaar, et al., Radiomics: extracting more information from medical images using advanced feature analysis, Eur. J. Cancer 48 (4) (2012) 441–446.
[12] P Lambin, RTH Leijenaar, TM Deist, et al., Radiomics: the bridge between medical imaging and personalized medicine, Nat. Rev. Clin. Oncol. 14 (12) (2017) 749–762.
[13] T Wakabayashi, F Ouhmich, C Gonzalez-Cabrera, et al., Radiomics in hepatocellular carcinoma: a quantitative review, Hepatol. Int. (2019).
[14] HJ Park, JH Kim, SY Choi, et al., Prediction of therapeutic response of hepatocellular carcinoma to transcatheter arterial chemoembolization based on pretherapeutic dynamic CT and textural findings, AJR Am. J. Roentgenol. 209 (4) (2017) W211–Ww20.
[15] J Kim, SJ Choi, SH Lee, HY Lee, H. Park, Predicting survival using pretreatment CT for patients with hepatocellular carcinoma treated with transarterial chemoembolization: comparison of models using radiomics, AJR Am. J. Roentgenol. 211 (5) (2018) 1026–1034.
[16] XP Meng, YC Wang, S Ju, et al., Radiomics analysis on multiphase contrast-enhanced CT: a survival prediction tool in patients with hepatocellular carcinoma undergoing transarterial chemoembolization, Front Oncol 10 (2020) 1196.
[17] KM Elsayes, AZ Kielar, MM Elmohr, et al., White paper of the Society of Abdominal Radiology hepatocellular carcinoma diagnosis disease-focused panel on LI-RADS v2018 for CT and MRI, Abdominal Radiol. (New York) 43 (10) (2018) 2625–2642.
[18] N Yoneda, O Matsui, S Kobayashi, et al., Current status of imaging biomarkers predicting the biological nature of hepatocellular carcinoma, Jpn J. Radiol. 37 (3) (2019) 191–208.
[19] P Yushkevich, J Piven, H Hazlett, et al., User-guided 3D active contour segmentation of anatomical structures: significantly improved efficiency and reliability, Neuroimage 31 (3) (2006) 1116–1128.
[20] JJM van Griethuysen, A Fedorov, C Parmar, et al., Computational radiomics system to decode the radiographic phenotype, Cancer Res. 77 (21) (2017) e104–e1e7.
[21] Y Song, J Zhang, Y Zhang, et al., FeAture Explorer (FAE): a tool for developing and comparing radiomics models, PLoS One 15 (8) (2020) e0237587.
[22] M Kudo, K Ueshima, M Ikeda, et al., Randomised, multicentre prospective trial of transarterial chemoembolisation (TACE) plus sorafenib as compared with TACE alone in patients with hepatocellular carcinoma: TACTICS trial, Gut 69 (8) (2019) gutjnl-2019-318934.
[23] M Kudo, O Matsui, N Izumi, et al., JSH consensus-based clinical practice guidelines for the management of hepatocellular carcinoma: 2014 update by the liver cancer study group of Japan, Liver Cancer 3 (3-4) (2014) 458–468.
[24] F Hucke, M Pinter, I Graziadei, et al., How to STATE suitability and START transarterial chemoembolization in patients with intermediate stage hepatocellular carcinoma, J. Hepatol. 61 (6) (2014) 1287–1296.
[25] A Mahringer-Kunz, R Kloeckner, MB Pitton, et al., Validation of the risk prediction models STATE-score and START-strategy to guide TACE treatment in patients with hepatocellular carcinoma, Cardiovasc Intervent Radiol 40 (7) (2017) 1017–1025.
[26] RS Finn, S Qin, M Ikeda, et al., Atezolizumab plus bevacizumab in unresectable hepatocellular carcinoma, N. Engl. J. Med. 382 (20) (2020) 1894–1905.
[27] K Katayama, T Imai, Y Abe, et al., Number of nodules but not size of hepatocellular carcinoma can predict refractoriness to transarterial chemoembolization and poor prognosis, J. Clin. Med. Res. 10 (10) (2018) 765–771.
[28] LQ Dong, LH Peng, LJ Ma, et al., Heterogeneous immunogenomic features and distinct escape mechanisms in multifocal hepatocellular carcinoma, J. Hepatol. 72 (5) (2020) 896–908.
[29] L Xu, ZW Peng, MS Chen, et al., Prognostic nomogram for patients with unresectable hepatocellular carcinoma after transcatheter arterial chemoembolization, J. Hepatol. 63 (1) (2015) 122–130.
[30] MY Hsieh, WY Chang, LY Wang, et al., Treatment of hepatocellular carcinoma by transcatheter arterial chemoembolization and analysis of prognostic factors, Cancer Chemother. Pharmacol. 31 (Suppl) (1992) S82–S85.
[31] PJ Johnson, S Berhane, C Kagebayashi, et al., Assessment of liver function in patients with hepatocellular carcinoma: a new evidence-based approach-the ALBI grade, J. Clin. Oncol. 33 (6) (2015) 550–558.